Differentiable Physics and Graph Representations for Kirigami Form Finding

Julien Kloers[1,2], Dr. R. Pastrana[3], Prof. S. Adriaenssens[1]

PRINCETON UNIVERSITY

Problem Statement : Kirigami & Physics

Kirigami mechanics pose a highly non-linear, discrete physical problem that couples topology and geometry. We define a *valid* kirigami $X \in \mathcal{K}$ as a mechanism kinematically capable of continuously opening and closing. To ultimately generalize to 3D and aperiodic motifs, we first study Rigid Planar Quadrangular Deployable Kirigami (RP-QDK) [4].

Objective: Study the pipeline's ability to **match a target shape under external loads** starting from an initial deployed/folded configuration.

Exploring kirigami-energy space

The geometric space ($\mathcal{K}$) is high-dimensional, almost empty, and non-regular due to invalid configurations and face intersections, but differentiable almost everywhere, and the energy only makes sense on a valid geometry.

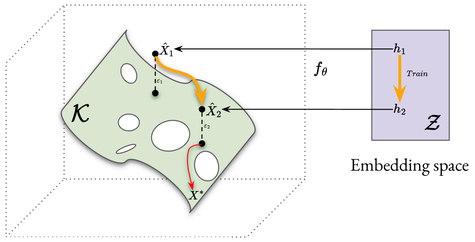

Figure 1. Topology of the valid Kirigami-Energy Space $\mathcal{K}$ and learning strategies. The initial guess $\hat{X}$ is projected onto the valid space before following a load-path (red curve) toward an optimum.

Physics Simulator

We adapted a static equilibrium solver based on a quasi-static hinge equilibrium model. [2] The internal energy relies on a hinge-based model computing Stretching, Bending, Shearing, and Contact Energy:

$$\mathcal{V}_i = \frac{1}{2}[k_t(\epsilon_i l_i^0)^2 + k_\theta \Delta\theta_i^2 + k_s(\psi_i l_i^0)^2] + \mathcal{V}_i^c$$

The potential energy of the system considering external work (forces, moments):

$$\Pi(t) = \sum_{i \in \text{hinges}} \mathcal{V}_i^t - \sum_{i \in \text{DOFs}} F_i^t u_i^t$$

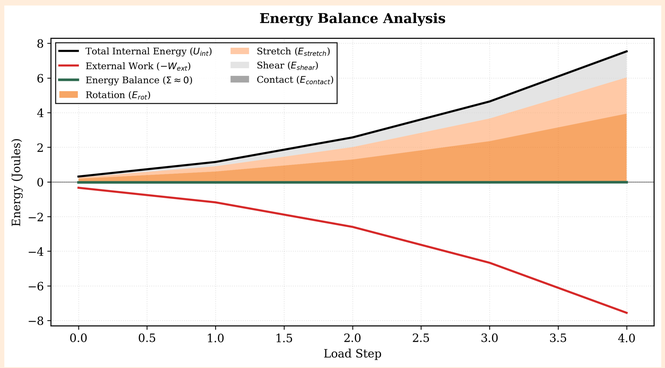

Figure 2. Energy Balance Analysis during the simulation.

Differentiable Physics Optimization Pipeline

We introduce an end-to-end differentiable pipeline that enables the inverse design of kirigami structures using gradient-based optimization in `JAX`.

Differentiable optimization

- **Initial map:** Makes the initial guess $\hat{X} = f_\theta(G, \mathcal{C})$
- **Validity solver:** Projects onto the valid kirigami space $X_{valid} = Proj_{\mathcal{K}}(\hat{X})$, [3]
- **Physics Simulator:** Follows the load-path $X_{load} = Sim(X_{valid}, F)$

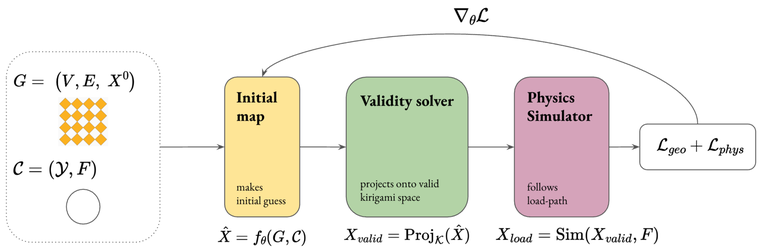

Figure 3. Overview of the optimization pipeline.

Learning the Initial Map

The initial map $\hat{X} = f_\theta(G, \mathcal{C})$ is a learnable function that maps the discrete topology (graph G) to the continuous physical domain ($\mathbb{R}^2$ or $\mathbb{R}^3$). It is critical for learning structural mechanics while remaining close to the valid manifold $\mathcal{K}$. The choice of the mapping family represents a trade-off between **expressivity** and **flexibility**.

Face centroids are mapped, while individual faces are rotated and scaled according to the transformation's **Jacobian matrix** J.

- **Algebraic (Baseline):** Capable of capturing basic geometry but lacks the flexibility to represent complex mechanical responses.
- **Conformal Polynomials (Proposed):** Analytically simple functions representing a broad family of transformations.

$$f'(z) = \prod_i \left(1 - w_i \frac{z}{r_i}\right)$$

  Optimizing singularities (r_i) and weights (w_i) allows the system to explore a wide range of initial configurations while maintaining local geometric consistency.
- **Neural (Future Work):** Directly learning the mapping through **GNNs**.

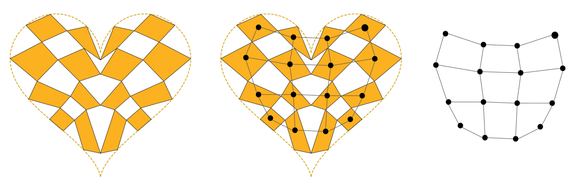

Figure 4. Dual graph of a regular 4×4 tessellation mapped to a heart-shaped target geometry.

The highly non-linear, constrained physics can be addressed by exploiting structural symmetries through Equivariant GNNs. Embedding nodes in space $\mathcal{Z}$ such that $f_\theta(\mathcal{Z}) \approx \mathcal{K}$ could allow for robust transformations / topology changes [1].

Matching Target Shape When Loaded

Experimental Results

We evaluate how different initial mapping strategies (Shirley-Chiu vs. Conformal Polynomials) influence the final equilibrium shape under various boundary conditions and external loads.

Protocol: We use 4×4 RP-QDK tessellations mapped from a deployed state to a circle in $\mathbb{R}^2$. Experiments incorporate symmetric and asymmetric loadings and clampings, including concentrated forces, moments, and combinations thereof.

Metrics: Strategies are compared based on *Shape Fidelity* (Chamfer distance to target), *Mechanical Validity* (Strain/Shear/Contact energy), and *Optimization Stability*.

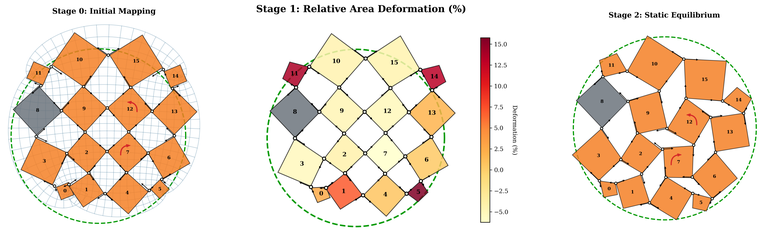

Figure 5. System evolution: Initial Mapping, Area Deformation, and Static Equilibrium.

Results: Learned maps discover lower-energy configurations, achieving a *65x improvement* in target matching accuracy (avg. Chamfer distance) compared to fixed analytic mappings.

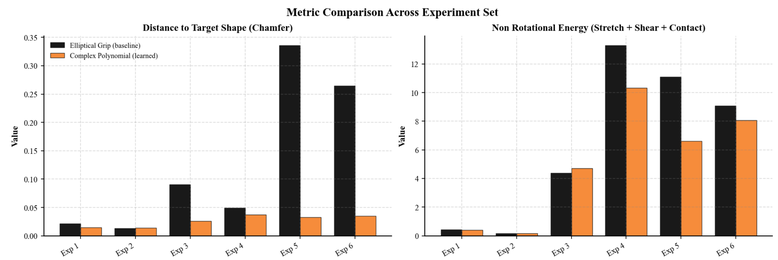

Figure 6. Performance comparison across loading protocols.

References

[1] Ilyes Batatia, Dávid Péter Kovács, Gregor N C Simm, Christoph Ortner, and Gábor Csányi. MACE: Higher order equivariant message passing neural networks for fast and accurate force fields.

[2] Giovanni Bordiga, Eder Medina, Sina Jafarzadeh, Cyrill Bösch, Ryan P. Adams, Vincent Tournat, and Katia Bertoldi. Automated discovery of reprogrammable nonlinear dynamic metamaterials. *Nature Materials*, 23(11):1486–1494, 2024.

[3] Gary P. T. Choi, Levi H. Dudte, and L. Mahadevan. Programming shape using kirigami tessellations. *Nature Materials*, 18(9):999–1004, 2019.

[4] Xiangxin Dang, Fan Feng, Huiling Duan, and Jianxiang Wang. Theorem for the design of deployable kirigami tessellations with different topologies. *Physical Review E*, 104(5):055006, 2021.

[1]Form Finding Lab, Princeton NJ [2]Ecole des Ponts, Paris [3]AI Lab, Princeton NJ